Department of Emergency Medicine Faculty Papers

Department of Emergency Medicine

4-1-2012

Essential role of caveolin-3 in adiponectin signalsome formation and adiponectin cardioprotection.

Yajing Wang
Shanxi Medical University; Thomas Jefferson University

Xiaoliang Wang
Shanxi Medical University; Thomas Jefferson University

Jean-François Jasmin
Thomas Jefferson University

Wayne Bond Lau
Thomas Jefferson University

Rong Li
Thomas Jefferson University

Recommended Citation

Authors

Yajing Wang, Xiaoliang Wang, Jean-François Jasmin, Wayne Bond Lau, Rong Li, Yuexin Yuan, Wei Yi, Kurt Chuprun, Michael P. Lisanti, Walter J Koch, Erhe Gao, and Xin-Liang Ma

Essential Role of Caveolin-3 in Adiponectin Signalsome Formation and Adiponectin Cardioprotection

Yajing Wang, Xiaoliang Wang, Jean-François Jasmin, Wayne Bond Lau, Rong Li, Yuexin Yuan, Wei Yi, Kurt Chuprun, Michael P. Lisanti, Walter J. Koch, Erhe Gao and Xin-Liang Ma

The online version of this article, along with updated information and services, is located on the
World Wide Web at:
http://atvb.ahajournals.org/content/32/4/934

Data Supplement (unedited) at:
http://atvb.ahajournals.org/content/suppl/2012/02/09/ATVBAHA.111.242164.DC1.html

Essential Role of Caveolin-3 in Adiponectin Signalsome Formation and Adiponectin Cardioprotection

Yajing Wang, Xiaoliang Wang, Jean-François Jasmin, Wayne Bond Lau, Rong Li, Yuexin Yuan, Wei Yi, Kurt Chuprun, Michael P. Lisanti, Walter J. Koch, Erhe Gao, Xin-Liang Ma

Objective—Adiponectin (APN) system malfunction is causatively related to increased cardiovascular morbidity/mortality in diabetic patients. The aim of the current study was to investigate molecular mechanisms responsible for APN transmembrane signaling and cardioprotection.

Methods and Results—Compared with wild-type mice, caveolin-3 knockout (Cav-3KO) mice exhibited modestly increased myocardial ischemia/reperfusion injury (increased infarct size, apoptosis, and poorer cardiac function recovery; $P<0.05$). Although the expression level of key APN signaling molecules was normal in Cav-3KO, the cardioprotective effects of APN observed in wild-type were either markedly reduced or completely lost in Cav-3KO. Molecular and cellular experiments revealed that APN receptor 1 (AdipoR1) colocalized with Cav-3, forming AdipoR1/Cav-3 complex via specific Cav-3 scaffolding domain binding motifs. AdipoR1/Cav-3 interaction was required for APN-initiated AMP-activated protein kinase (AMPK)–dependent and AMPK-independent intracellular cardioprotective signalings. More importantly, APPL1 and adenylate cyclase, 2 immediately downstream molecules required for AMPK-dependent and AMPK-independent signaling, respectively, formed a protein complex with AdipoR1 in a Cav-3 dependent fashion. Finally, pharmacological activation of both AMPK plus protein kinase A significantly reduced myocardial infarct size and improved cardiac function in Cav-3KO animals.

Conclusion—Taken together, these results demonstrated for the first time that Cav-3 plays an essential role in APN transmembrane signaling and APN anti-ischemic/cardioprotective actions. (*Arterioscler Thromb Vasc Biol*. 2012;32: 934-942.)

Key Words: cytokines ■ diabetes mellitus ■ reperfusion injury ■ signal transduction

Ischemic heart disease is the leading cause of death in patients with diabetes. Hyperglycemia and hyperlipidemia not only cause vascular injury resulting in myocardial ischemia but also directly adversely impact ischemic cardiomyocytes, causing larger infarct size, and more severe heart failure after myocardial ischemia.[1] Defining the molecular basis linking diabetes and ischemic heart disease may help in identifying novel therapeutic targets that will not only reduce myocardial infarction risk but also decrease cardiovascular mortality in diabetic patients.

Adiponectin (APN) is an adipocytokine secreted from adipose tissue. Clinical and experimental studies have demonstrated the potency of APN as an endogenous cardiovascular protective molecule. Reduced APN levels in type-2 diabetic patients not only contribute to increased vascular injury and MI morbidity but also play a causative role in increased cardiomyocyte death, and greater mortality in diabetic individuals post-MI.[2–5] However, knowledge of the molecular mechanisms responsible for APN-induced cardiomyocyte protection against MI injury remains elusive. More importantly, although several putative APN receptors have been proposed, transmembrane signaling mechanisms responsible for APN′s cardiomyocyte-protective effect remain undefined.

Caveolae are small, flask-like invaginations of the plasma membrane that create signaling microdomains, thereby providing spatial and temporal organization of cellular signaling events. Caveolins, the structural proteins found in caveolae, serve as scaffolds and regulators of signaling proteins.[6] Many signaling molecules compartmentalize within caveolae and interact with the scaffolding domain of caveolins. Numerous studies have demonstrated that caveolin scaffolding domain binding inhibits the function of multiple caveolar proteins involved in cell growth and proliferation.[7] Thus, caveolin has

been generally recognized as a signal inhibitor and a potent growth suppressor. However, recent studies have suggested that insulin signaling may be an exception, which requires the presence of caveolin for transmembrane signaling.[8] Numerous studies have demonstrated that APN shares many biological functions with insulin, including glucose uptake, lipid oxidation, and cardiovascular protection.[9,10] However, the role of caveolin in APN transmembrane signaling, ie, functioning as either an inhibitor or activator, has never been previously investigated.

Therefore, the aims of the present study were to (1) determine the role of caveolin-3 (Cav-3) (the predominant form of caveolin expressed in cardiomyocytes) in the cardioprotective actions of APN, and (2) investigate the molecular mechanisms responsible for Cav-3 regulation of APN transmembrane signaling.

Materials and Methods

All experiments were performed on adult (8–10 weeks) male Cav-3 knockout (Cav-3KO) mice or male wild-type (WT) littermate controls. Generation and characterization of Cav-3KO mice have been previously described.[11] The experiments were performed in adherence with the National Institutes of Health *Guide for the Care and Use of Laboratory Animals* and were approved by the Thomas Jefferson University Committee on Animal Care.

Mice were anesthetized with 2% isoflurane, and myocardial ischemia (MI) was produced by temporarily exteriorizing the heart via a left thoracic incision and placing a 6-0 silk suture slipknot around the left anterior descending coronary artery.[5] Twenty minutes after MI, animals were randomized to receive either vehicle or globular domain of APN (2 μg/g, IP).[5] After 30 minutes of MI, the slipknot was released, and the myocardium was reperfused for 3 hours or 24 hours (cardiac function and infarct size only). All assays were performed using tissue from ischemic/reperfused area or area at risk identified with Evens blue negative staining.

Cardiac function was determined by echocardiography (VisualSonics VeVo 770) and left ventricular (LV) catheterization (Millar 1.2-Fr micromanometer) methods 24 hours after reperfusion and before chest reopening.[5] Myocardial apoptosis was determined by caspase-3 activity and expressed as nmol of pNA/hour per mg of protein.[5] Total nitric oxide content (SIEVER 280i chemiluminescence NO Analyzer), superoxide production (lucigenin-enhanced chemiluminescence), and nitrotyrosine content (ELISA) in cardiac tissue were determined as we previously published.[12–14] Sucrose density membrane fractionation, immunoblotting, coimmunoprecipitation, adult mouse cardiomyocyte culture, and confocal microscopic analysis were all performed using standard methods from our laboratory[5] or other investigators. Detailed methods for all of the assays described above, as well as the methods for plasmid production and cell transfection, are provided in the online-only Data Supplement.

All values in the text and figures are presented as means$\pm$SEM of n independent experiments. All data (except Western blot density) were subjected to 2-way ANOVA followed by Bonferroni correction for post hoc test. Western blot densities were analyzed with the Kruskal-Wallis test followed by Dunn's post hoc test. Probabilities of 0.05 or less were considered statistically significant.

Results

Knockout of Cav-3 Modestly Increased Myocardial Ischemia/Reperfusion Injury but Virtually Abolished the Cardioprotection of APN

To definitively determine the role of Cav-3 in APN-mediated cardioprotection, the effect of APN on myocardial infarct size was determined in Cav-3KO mice and their WT littermates.

As summarized in Figure 1A, administration of APN 10 minutes before reperfusion significantly decreased infarct size in WT mice ($P<0.01$). Compared with WT mice, Cav-3KO mice exhibited moderately increased infarct size ($P<0.05$). Most importantly, administration of APN to Cav-3KO mice only slightly reduced infarct size. A highly significant difference in infarct size between APN-treated WT mice and APN-treated Cav-3KO mice was observed ($P<0.01$). The loss of APN-mediated protection in Cav-3KO mice cannot be attributed to reduced APN concentration in these animals ($P<0.05$),[11] as treatment with a tripled dose of APN (ie, 6 μg/g body weight) remained ineffective in reducing infarct size. Moreover, the loss of APN cardioprotection in Cav-3KO mice cannot be explained by a modestly larger infarct size observed in Cav-3KO mice, because we have recently demonstrated that APN is highly effective in protecting heart from myocardial ischemia/reperfusion (MI/R) injury in APN knockout mice, an animal model in which infarct size is even larger than that seen in Cav-3KO mice.[5] Finally, to determine whether Cav-3 is also required for cardioprotective action of full-length APN, HEK cell-produced full-length APN (>80% in high molecular weight format as certified by the manufacturer, BioVendor, Candler, NC) was administered at 10 μg/g (a dose that exerts comparable cardioprotection in WT animal as 2 μg/g globular APN). As summarized in Figure I in the online-only Data Supplement, the cardioprotective effect of full-length APN observed in WT mice was virtually abolished in Cav-3KO animals. These results demonstrated that Cav-3 is an essential molecule in APN-mediated cardioprotection.

Apoptosis plays a critical role in MI/R injury. To determine whether Cav-3 is also required in APN-mediated antiapoptotic signaling, the effect of APN on MI/R-induced caspase-3 activation was determined. Compared with WT mice, MI/R-induced caspase-3 activation was significantly increased in Cav-3KO mice. More importantly, the antiapoptotic effect of APN observed in WT mice was markedly, although not completely, blocked in Cav-3KO mice (Figure 1B). The difference in caspase-3 activity between APN-treated WT and APN-treated Cav-3KO mice was markedly significant ($P<0.01$).

Echocardiography and LV catheterization were used 24 hours after reperfusion to ascertain whether the beneficial effects of APN on cardiac function were Cav-3 dependent. As illustrated in Figure 1C and summarized in Figure 1D, MI/R caused greater LV dysfunction in Cav-3KO mice than WT ($P<0.05$). Although APN treatment significantly improved LV function in WT mice, the same treatment failed to improve LV function to significant extent in Cav-3KO mice (Figure 1C and 1D). As seen with echocardiography, Cav-3KO mice manifested significantly poorer cardiac function by LV catheterization, as evidenced by higher LV end diastolic pressure and lower $\pm$dP/dt$_{max}$ (Figure 1E and 1F). Treatment of WT mice with APN significantly reduced LV end diastolic pressure ($P<0.01$) and improved $\pm$dP/dt$_{max}$ ($P<0.01$). However, the beneficial effects of APN on cardiac function were either markedly reduced or completely lost in Cav-3KO mice. There was a highly significant difference in
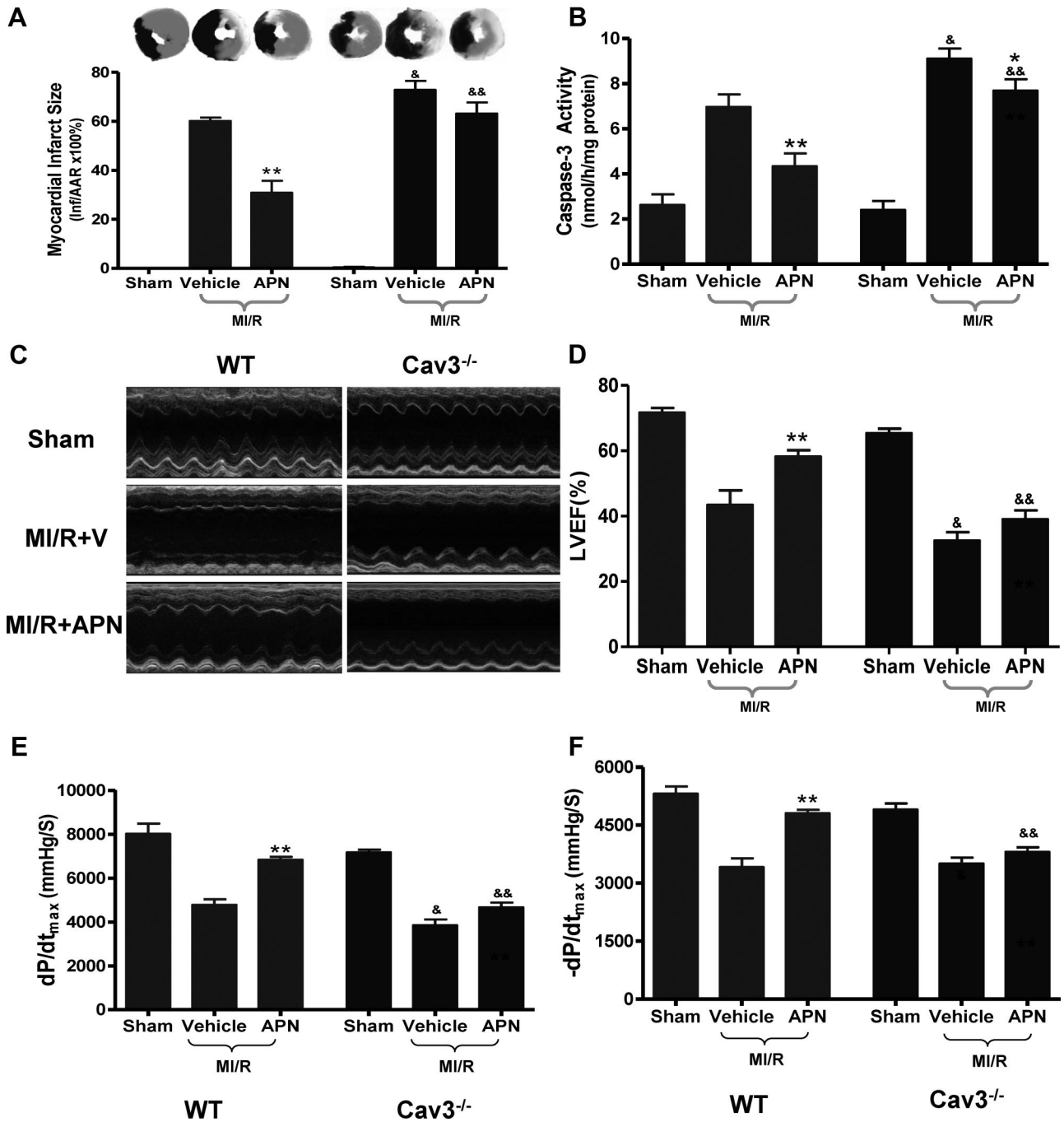
Figure 1. Knockout of Cav-3 abolished APN's infarct size sparing effect (**A**), markedly blunted APN's antiapoptotic effect (**B**), and abolished APN's cardiac functional improvement effect as determined by LVEF (**C** and **D**) and $\pm dP/dt_{max}$ (**E** and **F**). n=12 to 15/group. *$P<0.05$, **$P<0.01$ vs the respective vehicle group; &$P<0.05$, &&$P<0.01$ vs WT mice with the same treatment in ischemic/reperfused heart. n=12 to 15/group. APN indicates adiponectin; Cav3, caveolin-3; LVEF, left ventricular ejection fraction; MI/R, myocardial ischemia/reperfusion; V, vehicle; WT, wild-type.

$\pm dP/dt_{max}$ between APN-treated WT mice and APN-treated Cav-3KO mice (Figure 1E and 1F).

APN Signaling Machinery Is Intact in Cav-3KO Mice

The above results clearly demonstrate that Cav-3 is required for APN-mediated cardioprotective signaling. To determine the mechanisms responsible for the loss of APN-mediated cardioprotection in Cav-3KO mice, we first assessed the state

of molecules requisite for physiological APN biological signaling. No difference in cardiac expression of APN receptor (AdipoR)-1, AdipoR2, APPL1 (an adaptor protein containing a phosphotyrosine binding domain, a pleckstrin homology domain, and a leucine zipper motif), or AMP-activated protein kinase (AMPK) was observed between WT and Cav-3KO mice (Figure I in the online-only Data Supplement). These results demonstrate that the loss of APN-mediated cardioprotection in Cav-3KO mice cannot be attrib-
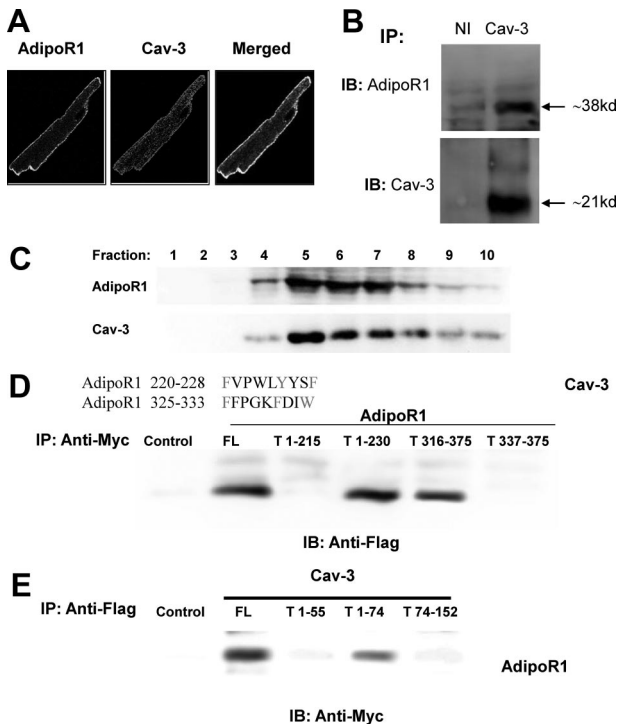
Figure 2. AdipoR1 colocalized (**A**) and interacted with caveolin-3 (Cav-3) (**B**). **C**, AdipoR1 was distributed in detergent-resistant (caveolae-rich) fractions (fractions 5 and 6), but not in detergent-soluble fractions. **D**, AdipoR1/Cav-3 interaction was detected in cells cotransfected with full-length Cav-3 plus full-length AdipoR1 (FL), truncated AdipoR1$^{1-230}$, or truncated AdipoR1$^{316-375}$ but not in cell lysates expressing truncated AdipoR1$^{1-215}$ or truncated AdipoR1$^{337-375}$. **E**, AdipoR1/Cav-3 interaction was detected in cells cotransfected with full-length AdipoR1 plus full-length Cav-3 (FL) or truncated Cav-3$^{1-74}$ but not in cell lysates expressing truncated Cav-3$^{1-55}$ or truncated Cav-3$^{74-151}$. For confocal microscopic examination, >100 cells were inspected per experiment, and cells with typical morphology are presented. For Western and coimmunoprecipitation, at least 6 samples from different tissue/cell culture dishes were examined, and typical blots are presented. IB indicates immunoblotting; IP, immunoprecipitation.

uted to the deficiency of key membrane or intracellular APN signaling molecules.

Colocalization and Interaction of AdipoR1 and Cav-3 in Adult Cardiomyocytes

Previous studies have demonstrated that caveolin interacts with many membrane receptors. Recent studies have demonstrated that APN receptors are 7-transmembrane domain proteins, but with structural and topologic distinction from G-protein–coupled receptors.[15] Having demonstrated that APN′s cardioprotection is abolished in Cav-3KO mice, we decided to test a novel hypothesis that interaction between AdipoR1, the predominant form of APN receptor in muscular cells, and Cav-3, the predominant form of caveolin in muscular cells, might be requisite for proper APN transmembrane signaling and cardioprotection. As illustrated in Figure 2A, AdipoR1 (green fluorescence) and Cav-3 (red fluorescence) were both confined to the plasma membrane. The image overlay demonstrates colocalization of AdipoR1 and Cav-3 (yellow staining). The staining was specific for AdipoR1 and Cav-3, because substitution of nonimmune IgG for Adi-poR1 and Cav-3.

AdipoR1 antibody yielded only red plasma membrane staining, and substitution of Cav-3 antibody with nonimmune IgG resulted in only AdipoR1 green staining (data not shown). To determine whether there is an interaction between Cav-3 and AdipoR1, cardiac lysates were immunoprecipitated with an antibody directed against Cav-3 or a nonimmune IgG, and AdipoR1/Cav-3 proteins in the precipitates were detected by Western blot analysis. As illustrated in Figure 2B, neither AdipoR1 nor Cav-3 protein was detected when samples were immunoprecipitated with a nonimmune IgG (left lanes). However, AdipoR1 was detected in lysates immunoprecipitated with antibody against Cav-3 (right lanes). Similarly, when cell lysates were immunoprecipitated with an antibody against AdipoR1, Cav-3 proteins were detected by Western blot analysis (data not shown). To confirm localization of AdiopR1 to caveolae and AdipoR1/Cav-3 complex formation in caveolae, a caveolae-rich detergent-resistant membrane fraction was prepared from adult heart tissues, and AdipoR1/Cav-3 distribution and interaction were detected by Western blotting and coimmunoprecipitation. As shown in Figure 2C, AdipoR1, and Cav-3 proteins were associated with the detergent-resistant membrane fraction. Moreover, AdipoR1/Cav-3 complex formation was clearly detected in the detergent-resistant membrane fraction (Figure II in the online-only Data Supplement, fractions 5 and 6) but not in detergent-soluble fractions (Figure II in the online-only Data Supplement, fractions 9 and 10).

AdipoR1 Binds to Cav-3 Scaffolding Domain via Specific Cav-3 Interaction Motif

Having demonstrated that AdipoR1 colocalizes and interacts with Cav-3, we further identified the specific domains responsible for AdipoR1/Cav-3 interaction. Previous experiments have demonstrated that membrane proteins interact with caveolin scaffolding domain via a specific caveolin-binding motif ($\varphi X\varphi XXXX\varphi$ or $\varphi XXXX\varphi XX\varphi$, φ being an aromatic residue). Sequence analysis revealed 2 potential caveolin-binding motifs in AdipoR1 (^{220}FVPWLYYSF^{228} and ^{325}FFPGKFDIW^{333}). To determine whether AdipoR1 binds Cav-3 via these specific motifs, vectors expressing myc-tag full-length AdipoR1 or truncated AdipoR1 (Figure III in the online-only Data Supplement) were cotransfected with flag-tag full-length Cav-3 into 293T cells. Cell lysates were immunoprecipitated with anti-myc antibody and immunoblotted with anti-flag antibody. As shown in Figure 2D, Cav-3 protein was detected in cell lysates expressing full-length AdiopR1, truncated AdipoR1$^{1-230}$, or truncated AdipoR1$^{316-375}$ but not in cell lysates expressing truncated AdipoR1$^{1-215}$ or truncated AdipoR1$^{337-375}$. These results demonstrate that AdipoR1 interacts with Cav-3 via the specific Cav-3 binding motif.

To further determine whether the Cav-3 scaffolding domain (residues 55–74) is required for AdipoR1 binding, vectors expressing full-length Cav-3 or truncated (Figure III in the online-only Data Supplement) Cav-3 were cotransfected with myc-tag full-length AdipoR1 into 293T cells. Cell lysates were immunoprecipitated with anti-flag antibody and immunoblotted with anti-myc antibody. As shown in Figure 2E, AdipoR1 protein was detected in cell lysates expressing

full-length Cav-3 or truncated Cav-3[1-74] but not in cell lysates expressing truncated Cav-3[1-55] or truncated Cav-3[74-151]. These results demonstrate that AdipoR1 specifically binds to the Cav-3 scaffolding domain.

Cav-3 Is Required for Both AMPK-Dependent and AMPK-Independent APN Cardioprotection

We and others have previously demonstrated that APN protects cardiomyocytes from ischemia/reperfusion injury via AMPK-dependent metabolic regulation, as well as AMPK-independent antioxidation/antinitration.[16] To further determine whether AdipoR1/Cav-3 interaction is required for AMPK-dependent or AMPK-independent intracellular cardioprotective signaling, the effect of APN on AMPK phosphorylation and nitrotyrosine content (an index for APN's AMPK-independent antioxidative/antinitrative properties[17]) were determined. As shown in Figure 3A and 3B, AMPK and acetyl-coenzyme A carboxylase phosphorylation was significantly increased after MI/R, and APN administration further augmented AMPK and acetyl-coenzyme A carboxylase phosphorylation in WT mice. Basal levels of AMPK phosphorylation and MI/R-induced AMPK phosphorylation were both slightly reduced (not statistically significant) in Cav-3KO mice. Most importantly, administration of APN failed to induce AMPK and acetyl-coenzyme A carboxylase phosphorylation in these mice (Figure 3A), indicating that Cav-3 is required for APN-induced AMPK activation.

Treatment of WT mice with APN significantly reduced nitrotyrosine content in the ischemic/reperfused heart (Figure 3C). Basal nitrotyrosine content was unaltered, but ischemia/reperfusion-induced nitrotyrosine formation was significantly increased in Cav-3KO mice. Treatment of Cav-3KO mice with APN failed to reduce nitrotyrosine content in the ischemic/reperfused heart. To further determine the arm of peroxynitrite overproduction (ie, overproduction of NO or superoxide) specifically inhibited by APN in a Cav-3 dependent fashion, NO/superoxide production and inducible nitric oxide synthase/phagocyte NADPH oxidase-2 (NOX)-2 (the prototypical and predominant form of NADPH oxidase in adult cardiomyocytes[18]) expressions were determined. In WT mice, APN significantly reduced ischemia/reperfusion-induced NO/superoxide production (Figure 4A and 4B) and inhibited inducible nitric oxide synthase/NOX-2 expression (Figure 4C and 4D). Knockout of Cav-3 further aggravated ischemia/reperfusion-induced NO/superoxide production (Figure 4A and 4B), and elevated NOX-2 expression (Figure 4D). Ischemia/reperfusion induced inducible nitric oxide synthase expression was slightly increased in the Cav-3KO heart (Figure 4C). In Cav-3KO mice, the inhibitory effect of APN on NO/superoxide production and NOX-2 overexpression was completely abolished, and the inhibitory effect of APN on inducible nitric oxide synthase expression was significantly blunted (Figure 4). Finally, congruent with previous reports, whereas basal endothelial nitric oxide synthase expression was unchanged, endothelial nitric oxide synthase phosphorylation was increased in Cav-3KO heart (Figure IV in the online-only Data Supplement). However, APN-induced endothelial nitric oxide synthase phosphorylation was abolished in Cav-3KO heart.
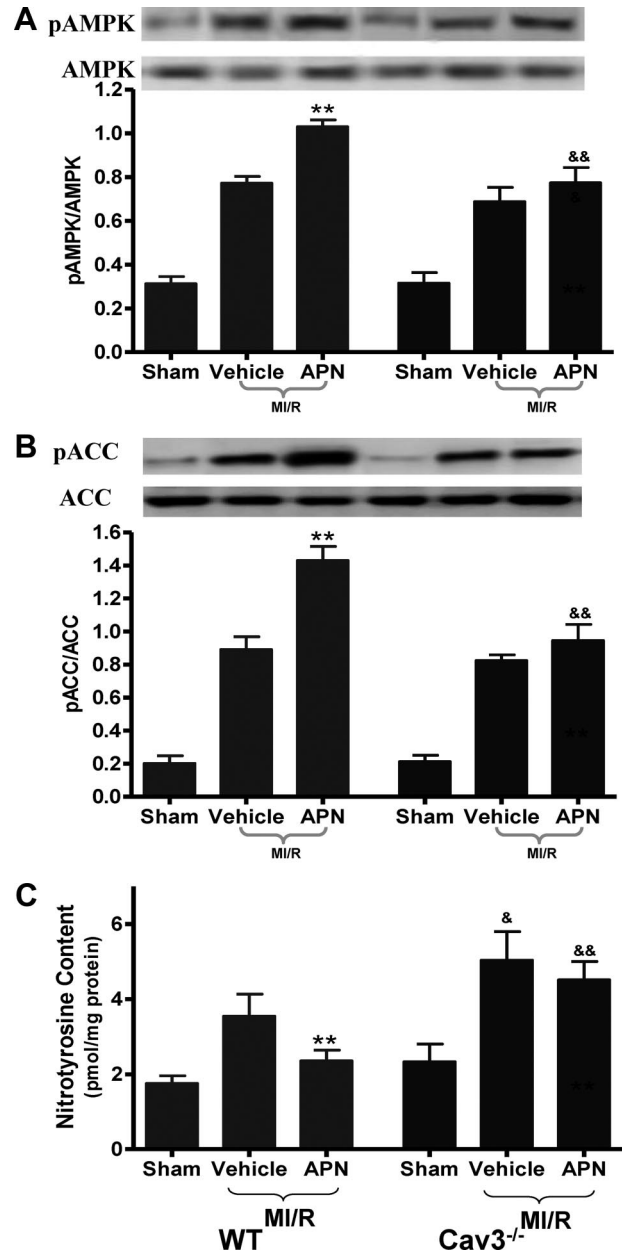
Figure 3. Knockout of Cav-3 abolished APN's AMPK (**A**) and ACC (**B**) activation and reduced its antinitrative effect (**C**). n=12 to 15/group. **$P<0.01$ vs the respective vehicle group; &$P<0.05$, &&$P<0.01$ vs wild-type (WT) mice with the same treatment. ACC indicates acetyl-coenzyme A carboxylase; AMPK, AMP-activated protein kinase; APN, adiponectin; Cav3, caveolin-3; MI/R, myocardial ischemia/reperfusion; pACC, phospho-acetyl-coenzyme A carboxylase; WT, wild-type.

AdipoR1 Interacts With APPL1 and Adenylate Cyclase in a Largely Cav3-Dependent Fashion

Recent studies suggest that APPL1 and adenylate cyclase (AC) are the most upstream signaling molecules in APN-induced AMPK activation and APN's antioxidative signaling, respectively.[16] Having demonstrated that Cav-3 is required for both AMPK activation and antioxidative signaling of APN, we investigated the relationships between AdipoR1, Cav-3, APPL1, and AC to explore the potential mechanism responsible for Cav-3-depedent APN transmembrane signaling. First, cardiac lysates were immunoprecipitated with an
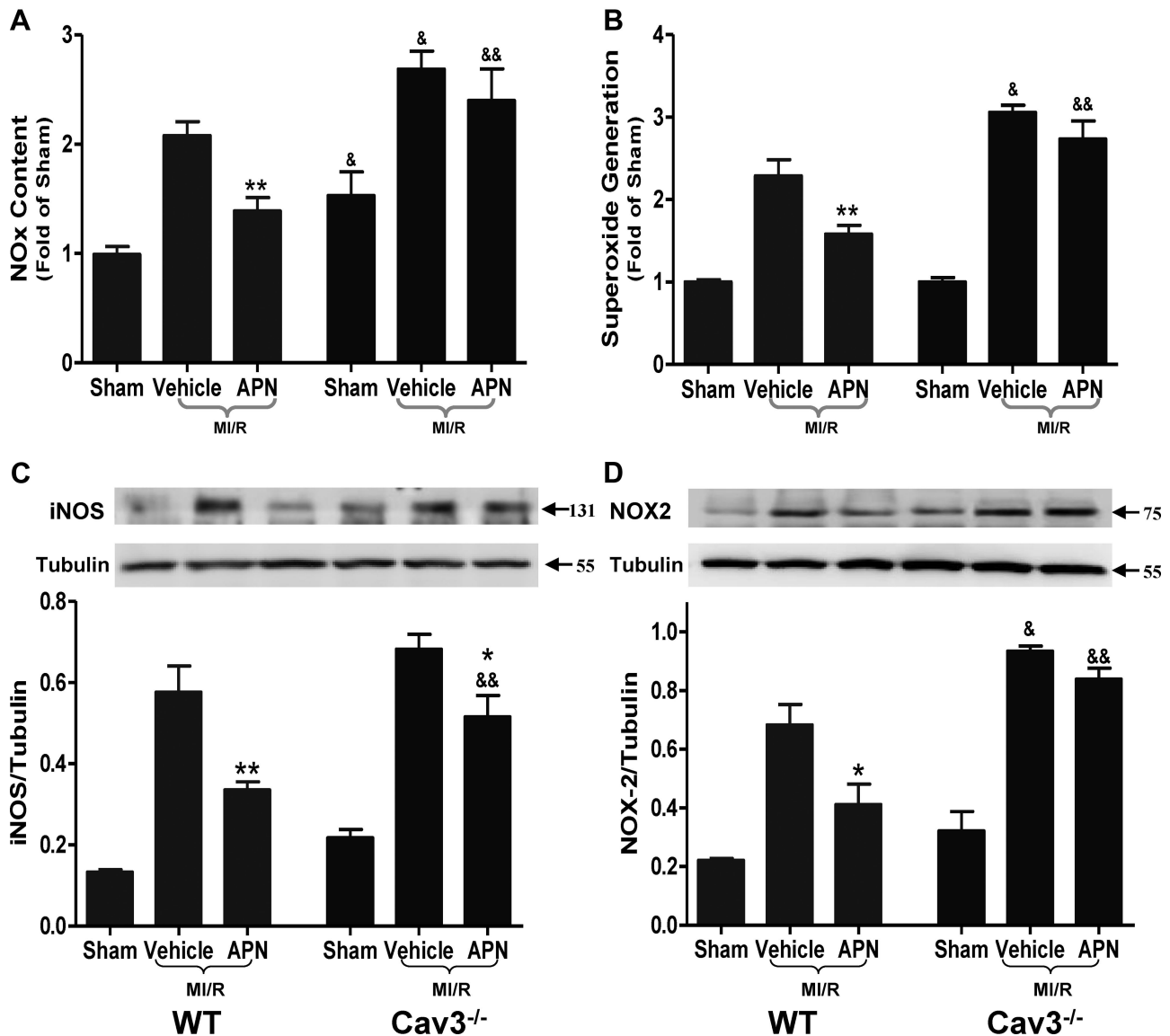
Figure 4. Knockout of Cav-3 abolished APN's antinitrative (determined by total NO production) (**A**) and antioxidative (determined by superoxide production [**B**] and phagocyte NADPH oxidase-2 (NOX) expression [**D**]) and markedly blunted APN's anti-iNOS effect (**C**) in ischemic/reperfused heart determined 3 hours after reperfusion. n=12 to 15/group. *$P<0.05$, **$P<0.01$ vs the respective vehicle group; &$P<0.05$, &&$P<0.01$ vs wild-type (WT) mice with the same treatment. APN indicates adiponectin; Cav3, caveolin-3; iNOS, inducible nitric oxide synthase; MI/R, myocardial ischemia/reperfusion; WT, wild-type.

antibody against Cav-3, and immunoblotted with an antibody against APPL1 or AC. As illustrated in Figure 5A, Cav-3 interacts with these 2 proteins to form a protein complex. Second, cardiac lysates were immunoprecipitated with an antibody against AdipoR1 and immunoblotted with an antibody against APPL1 or AC. Interestingly, both AdipoR1/APPL1 and AdipoR1/AC complex formation were also detected (Figure 5B). Finally, and most importantly, AdipoR1/APPL1 and AdipoR1/AC interactions were markedly reduced in Cav-3KO cardiac tissue (Figure 5B, demonstrating >80% reduction in 5 repeated experiments).

Cotreatment With an AMPK Activator and cAMP Mimic Significantly Reduced MI/R Injury in Cav-3KO Mice

The aforementioned results strongly suggest that via interaction with both AdipoR1 and its immediately downstream

signaling molecules, Cav-3 plays an essential role in APN signaling complex formation. To obtain further evidence supporting this novel hypothesis, additional experiments were performed. WT littermates or Cav-3KO mice were subjected to MI/R as described above and treated with either vehicle or AICAR (an AMPK activator, 300 µg/g, IP) plus N(6),2′-O-dibutyryladenosine 3′:5′ cyclic monophosphate (a cAMP mimic, 25 µg/g, IP). Dosages of AICAR and N(6),2′-O-dibutyryladenosine 3′:5′ cyclic monophosphate were selected from previous publications, and confirmed in a pilot experiment demonstrating that treatment with these 2 compounds in Cav-3KO mice resulted in AMPK and protein kinase A activation comparable to that seen in WT mice treated with APN (data not shown). As summarized in Figure 5C and 5D, although MI/R injury N(6),2′-O-dibutyryladenosine 3′:5′ cyclic monophosphate cotreatment remained highly effective
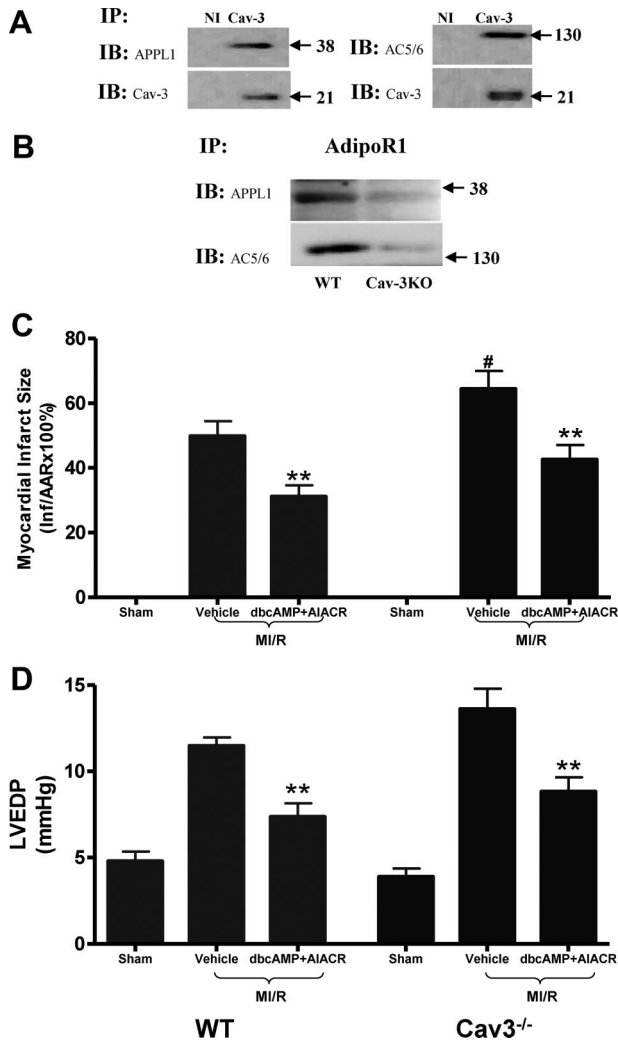
Figure 5. A, Cav-3 interacts with APPL1 (left) and AC (right) to form protein complex. **B,** AdipoR1/APPL1 and AdipoR1/AC complex formation was detected in tissue samples from wild-type (WT). These interactions were markedly reduced in Cav-3 knockout (Cav-3KO) cardiac tissue (>80% reduction in 5 repeated experiments). Administration of AICAR (an AMP-activated protein kinase [AMPK] activator) plus db-cAMP (a cAMP mimic) significantly reduced infarct size (**C**) and improved cardiac function (**D**) in Cav-3KO mice. AAR indicates area at risk; AC, adenylate cyclase; Cav-3, caveolin-3; Cav-3KO, caveolin-3 knockout; IB, immunoblotting; IP, immunoprecipitation; MI/R, myocardial ischemia/reperfusion; Inf, infarct; dbcAMP, N(6),2'-O-dibutyryladenosine 3':5' cyclic monophosphate, WT, wild-type.

in reducing infarct size and improving cardiac function in Cav-3KO mice. This result provided additional evidence that the loss of cardioprotection of APN in Cav3-KO mice is not the result of more severe MI/R injury in these animals.

T-Cadherin Localizes in Caveolae-Rich Membrane Fraction of Cardiomyocytes but Does Not Interact With AdipoR1 or Cav-3

A recent study demonstrated that T-cadherin is critical for binding and protective functions of high molecular weight APN in cardiac myocytes.[19] To determine whether T-cadherin expression is changed in Cav-3KO mice and whether T-cadherin may interact with AdipoR1/Cav-3 com-
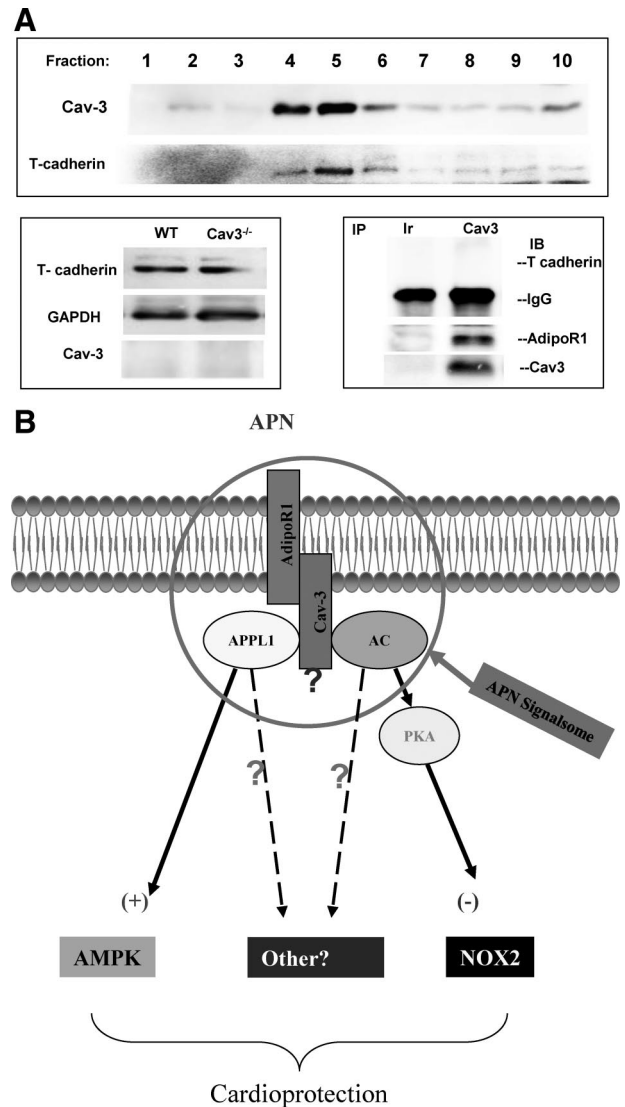
Figure 6. A, Comparison of T-cadherin expression in wild-type (WT) and caveolin-3 (Cav-3) knockout (Cav-3KO) heart, and determination of T-cadherin distribution and its interaction with AdipoR1 or Cav-3. **B,** Schematic illustration revealing the role of Cav-3 in adiponectin (APN) signalsome formation and APN cardioprotective signaling. **Solid lines:** established signaling pathways; **dashed lines:** pathways requiring additional investigation. Blue question mark indicates other intracellular APN signaling molecules that may also be "tethered" by Cav-3. AC indicates adenylate cyclase; APN, adiponectin; Cav-3, caveolin-3; IB, immunoblotting; IP, immunoprecipitation; Ir, irrelevant; PKA, protein kinase A; WT, wild-type.

plex, an additional experiment was performed. Interestingly, T-cadherin is distributed in detergent-insoluble, caveolae-rich membrane fraction (Figure 6A, top). However, T-cadherin expression was not changed in Cav-3KO heart (Figure 6A, second panel, left half). No interaction between T-cadherin and AdipoR1 or Cav-3 was detected (Figure 6A, second panel, right half).

Discussion

APN regulates cellular function via binding and activation of APN receptors (AdipoR), including AdipoR1 and AdipoR2.[15] In addition to these 2 receptors, cell surface calreticulin/CD91

coreceptor has been shown to be the molecule responsible for COX-2 activation by APN in endothelial cells.[20] Moreover, T-cadherin has been proposed to be a receptor for hexameric and high-molecular-weight forms of APN.[21] However, T-cadherin lacks an intracellular domain and is mostly likely important in tethering high molecular weight APN isoforms on the cell surface, thus allowing their interaction with other receptors.[19] The intracellular signaling of APN has been extensively investigated in recent years. At least 3 pathways, including the AMPK/acetyl-coenzyme A carboxylase signaling axis,[22] AMPK/endothelial nitric oxide synthase axis,[23,24] and AC/cAMP/protein kinase A signaling axis[16,17] have been reported. However, how the APN signal is transduced from its receptor(s) to intracellular effectors remains largely unknown. APPL1 is the only intracellular signaling molecule identified thus far with ability to shuttle signaling from AdipoR1 to intracellular effectors.[10,25] However, questions remain incompletely answered. Although the phosphotyrosine binding domain within APPL1 is absolutely required for APPL1/AdipoR1 interaction, no phosphorylated tyrosine residue is identified on AdipoR1 either before or after APN receptor binding. Additionally, only 1-way translocation of APPL1 (ie, from membrane to cytosol but not reversely) has been observed after APN/receptor binding, suggesting that those APPL1 proteins already present in close proximity to AdipoR1 are the molecules responsible for APN signaling propagation from membrane to intracellular effectors.

The most important finding of the present study is that Cav-3 interacts with AdipoR1, as well as APPL1 (the most important molecule in APN′s AMPK-dependent signaling) and AC (the most important molecule in APN′s AMPK-independent signaling), forming a signaling complex (signalsome) within caveolae. By interacting with AdipoR1 and key intracellular APN signaling molecules, Cav-3 corrals such downstream molecules in close proximity with AdipoR1, thus enabling proper transmembrane signaling and cardioprotection (Figure 6B). Functionally, this AdipoR1/Cav-3 interaction is similar to that of the insulin receptor/caveolin interaction.[11,26–28] However, a difference exists. In Cav-1 knockout adipocytes, insulin receptor mRNA levels are not changed, but insulin receptor protein content is markedly decreased, suggesting that Cav-1 stabilizes insulin receptor and inhibits its degradation.[29] However, our present experiments yielded no significant change in AdipoR1/2 expression in Cav-3KO cardiomyocytes at either the mRNA level or the protein level, suggesting the existence of more complex mechanisms responsible for Cav-3 regulation of AdipoR1 signaling.

Although both Cav-1KO and Cav-3KO mice manifest reduced insulin response, only Cav-3KO mice exhibit typical type-2 diabetic changes, including increased adiposity, decreased glucose uptake, reduced skeletal muscle glucose metabolic flux, and increased plasma leptin levels.[11] Importantly, older Cav-3-null mice develop pathological cardiac phenotypes, including cardiac hypertrophy and heightened ERK1/2 activation. However, Cav-3KO mice at age 2 months (as in the current study) do not exhibit any myopathic changes.[11] Additionally, several recent studies have demonstrated that Cav-3 is positively involved in post-MI cardioprotection.[30–32] Moreover, although increased MI/R injury

has been reported in both Cav-1KO and Cav-3KO mice in vivo, our most recent preliminary data obtained in cultured cardiomyocytes demonstrate that APN′s transmembrane signaling is impaired in Cav-3, but not Cav-1, knockdown cardiomyocytes. In contrast, Cav-1 knockdown in endothelial cells significantly blocks APN transmembrane signaling. Together, these results suggest that lack of Cav-1, an endothelial cell caveolin subtype, may increase MI/R injury indirectly by impairing blood flow restoration after reperfusion. In contrast, lack of Cav-3, a muscle-cell specific caveolin subtype, impairs APN transmembrane signaling in cardiomyocytes, directly augmenting MI/R injury.

It should be indicated that Cav-3KO markedly, but not completely, abolished all biological functions of APN, including a small portion of antiapoptotic effect (Figure 1B) and AMPK activating effect (Figure 3C). A previous study has demonstrated that AdipoR1 interacts with APPL1 and activates AMPK.[25] As shown in Figure 5B, AdipoR1/APPL1 interaction is markedly reduced but not completely lost in Cav-3KO cardiomyocytes. The remaining (approximately 20%) direct AdipoR1/APPL1 could be responsible for the small portion of AMPK activation by APN in Cav-3KO mice. In addition, although AdipoR1 is the predominant APN receptor expressed in cardiomyocytes, low levels of AdipoR2 are expressed in cardiomyocytes. Sequence analysis revealed that AdipoR2 contains 1 potential caveolin-binding motif that is located in its transmembrane domain. No significant AdipoR2/Cav-3 interaction was detected in our pilot experiment. A small portion of biological function of APN remaining in Cav-3KO mice could also be partially attributed to AdipoR2 activation and signaling. As systemic APN malfunction has been identified as a major risk factor for increased cardiovascular morbidity and mortality in type-2 diabetics, detailed elucidation of the signaling cascade mediated by the AdipoR1/Cav-3 interaction will not only gain comprehension of the APN signaling pathway and its regulation, but also provide valuable information on the design of new pharmacological interventions for clinically important diseases, such as obesity and type-2 diabetes.

While this article was in the final stages of preparation, an excellent study was published reporting that APN activates ceramidase in receptor-dependent fashion, initiating the pleiotropic actions of APN.[33] Our most recent experimental results demonstrate that although ceramidase is not a component of the Cav-3 centered APN signalsome during resting conditions, Cav-3 plays an essential role in APN-induced ceramidase recruitment and activation. Experiments identifying the role of Cav-3 in APN-initiated ceramidase recruitment/activation, and the involved detailed molecular mechanisms, are currently in progress.

Disclosures

None.

References

1. Norhammar A, Lindback J, Ryden L, Wallentin L, Stenestrand U. Improved but still high short- and long-term mortality rates after myocardial infarction in patients with diabetes mellitus: a time-trend report from the Swedish Register of Information and Knowledge about Swedish Heart Intensive Care Admission. *Heart*. 2007;93:1577–1583.

2. Basu R, Pajvani UB, Rizza RA, Scherer PE. Selective downregulation of the high molecular weight form (HMW) of adiponectin in hyperinsulinemia and in type 2 diabetes: differential regulation from non-diabetic subjects. *Diabetes*. 2007;56:2174–2177.

3. Ouchi N, Shibata R, Walsh K. Cardioprotection by adiponectin. *Trends Cardiovasc Med*. 2006;16:141–146.

4. Shibata R, Sato K, Pimentel DR, Takemura Y, Kihara S, Ohashi K, Funahashi T, Ouchi N, Walsh K. Adiponectin protects against myocardial ischemia-reperfusion injury through AMPK- and COX-2-dependent mechanisms. *Nat Med*. 2005;11:1096–1103.

5. Tao L, Gao E, Jiao X, Yuan Y, Li S, Christopher TA, Lopez BL, Koch W, Chan L, Goldstein BJ, Ma XL. Adiponectin cardioprotection after myocardial ischemia/reperfusion involves the reduction of oxidative/nitrative stress. *Circulation*. 2007;115:1408–1416.

6. Chidlow JH Jr, Sessa WC. Caveolae, caveolins, and cavins: complex control of cellular signalling and inflammation. *Cardiovasc Res*. 2010;86:219–225.

7. Schwencke C, Braun-Dullaeus RC, Wunderlich C, Strasser RH. Caveolae and caveolin in transmembrane signaling: implications for human disease. *Cardiovasc Res*. 2006;70:42–49.

8. Ishikawa Y, Otsu K, Oshikawa J. Caveolin; different roles for insulin signal? *Cell Signal*. 2005;17:1175–1182.

9. Berg AH, Combs TP, Scherer PE. ACRP30/adiponectin: an adipokine regulating glucose and lipid metabolism. *Trends Endocrinol Metab*. 2002;13:84–89.

10. Hosch SE, Olefsky JM, Kim JJ. APPLied mechanics: uncovering how adiponectin modulates insulin action. *Cell Metabolism*. 2006;4:5–6.

11. Capozza F, Combs TP, Cohen AW, Cho YR, Park SY, Schubert W, Williams TM, Brasaemle DL, Jelicks LA, Scherer PE, Kim JK, Lisanti MP. Caveolin-3 knockout mice show increased adiposity and whole body insulin resistance, with ligand-induced insulin receptor instability in skeletal muscle. *Am J Physiol Cell Physiol*. 2005;288:C1317–C1331.

12. Gao F, Gao E, Yue TL, Ohlstein EH, Lopez BL, Christopher TA, Ma XL. Nitric oxide mediates the antiapoptotic effect of insulin in myocardial ischemia-reperfusion: the roles of PI3-kinase, Akt, and endothelial nitric oxide synthase phosphorylation. *Circulation*. 2002;105:1497–1502.

13. Lund DD, Faraci FM, Miller FJ Jr, Heistad DD. Gene transfer of endothelial nitric oxide synthase improves relaxation of carotid arteries from diabetic rabbits. *Circulation*. 2000;101:1027–1033.

14. Ma XL, Gao F, Nelson AH, Lopez BL, Christopher TA, Yue TL, Barone FC. Oxidative inactivation of nitric oxide and endothelial dysfunction in stroke-prone spontaneous hypertensive rats. *J Pharmacol Exp Ther*. 2001;298:879–885.

15. Kadowaki T, Yamauchi T, Kubota N, Hara K, Ueki K, Tobe K. Adiponectin and adiponectin receptors in insulin resistance, diabetes, and the metabolic syndrome. *J Clin Invest*. 2006;116:1784–1792.

16. Goldstein BJ, Scalia RG, Ma XL. Protective vascular and myocardial effects of adiponectin. *Nat Clin Pract Cardiovasc Med*. 2009;6:27–35.

17. Wang Y, Gao E, Tao L, Lau WB, Yuan Y, Goldstein BJ, Lopez BL, Christopher TA, Tian R, Koch W, Ma XL. AMP-activated protein kinase deficiency enhances myocardial ischemia/reperfusion injury but has minimal effect on the antioxidant/antinitrative protection of adiponectin. *Circulation*. 2009;119:835–844.

18. Bedard K, Krause KH. The NOX family of ROS-generating NADPH oxidases: physiology and pathophysiology. *Physiol Rev*. 2007;87:245–313.

19. Denzel MS, Scimia MC, Zumstein PM, Walsh K, Ruiz-Lozano P, Ranscht B. T-cadherin is critical for adiponectin-mediated cardioprotection in mice. *J Clin Invest*. 2010;120:4342–4352.

20. Ohashi K, Ouchi N, Sato K, Higuchi A, Ishikawa TO, Herschman HR, Kihara S, Walsh K. Adiponectin promotes revascularization of ischemic muscle through a cyclooxygenase 2-dependent mechanism. *Mol Cell Biol*. 2009;29:3487–3499.

21. Hug C, Wang J, Ahmad NS, Bogan JS, Tsao TS, Lodish HF. T-cadherin is a receptor for hexameric and high-molecular-weight forms of Acrp30/adiponectin. *Proc Natl Acad Sci USA*. 2004;101:10308–10313.

22. Yamauchi T, Kamon J, Minokoshi Y, Ito Y, Waki H, Uchida S, Yamashita S, Noda M, Kita S, Ueki K, Eto K, Akanuma Y, Froguel P, Foufelle F, Ferre P, Carling D, Kimura S, Nagai R, Kahn BB, Kadowaki T. Adiponectin stimulates glucose utilization and fatty-acid oxidation by activating AMP-activated protein kinase. *Nat Med*. 2002;8:1288–1295.

23. Shibata R, Ouchi N, Kihara S, Sato K, Funahashi T, Walsh K. Adiponectin stimulates angiogenesis in response to tissue ischemia through stimulation of AMP-activated protein kinase signaling. *J Biol Chem*. 2004;279:28670–28674.

24. Chen H, Montagnani M, Funahashi T, Shimomura I, Quon MJ. Adiponectin stimulates production of nitric oxide in vascular endothelial cells. *J Biol Chem*. 2003;278:45021–45026.

25. Mao X, Kikani CK, Riojas RA, Langlais P, Wang L, Ramos FJ, Fang Q, Christ-Roberts CY, Hong JY, Kim RY, Liu F, Dong LQ. APPL1 binds to adiponectin receptors and mediates adiponectin signalling and function. *Nat Cell Biol*. 2006;8:518–523.

26. Gonzalez-Munoz E, Lopez-Iglesias C, Calvo M, Palacin M, Zorzano A, Camps M. Caveolin-1 loss-of-function accelerates GLUT4 and insulin receptor degradation in 3T3-L1 adipocytes. *Endocrinology*. 2009;150:3493–3502.

27. Oshikawa J, Otsu K, Toya Y, Tsunematsu T, Hankins R, Kawabe J, Minamisawa S, Umemura S, Hagiwara Y, Ishikawa Y. Insulin resistance in skeletal muscles of caveolin-3-null mice. *Proc Natl Acad Sci USA*. 2004;101:12670–12675.

28. Otsu K, Toya Y, Oshikawa J, Kurotani R, Yazawa T, Sato M, Yokoyama U, Umemura S, Minamisawa S, Okumura S, Ishikawa Y. Caveolin gene transfer improves glucose metabolism in diabetic mice. *Am J Physiol Cell Physiol*. 2010;298:C450–C456.

29. Cohen AW, Combs TP, Scherer PE, Lisanti MP. Role of caveolin and caveolae in insulin signaling and diabetes. *Am J Physiol Endocrinol Metab*. 2003;285:E1151–E1160.

30. Tsutsumi YM, Horikawa YT, Jennings MM, Kidd MW, Niesman IR, Yokoyama U, Head BP, Hagiwara Y, Ishikawa Y, Miyanohara A, Patel PM, Insel PA, Patel HH, Roth DM. Cardiac-specific overexpression of caveolin-3 induces endogenous cardiac protection by mimicking ischemic preconditioning. *Circulation*. 2008;118:1979–1988.

31. Horikawa YT, Panneerselvam M, Kawaraguchi Y, Tsutsumi YM, Ali SS, Balijepalli RC, Murray F, Head BP, Niesman IR, Rieg T, Vallon V, Insel PA, Patel HH, Roth DM. Cardiac-specific overexpression of caveolin-3 attenuates cardiac hypertrophy and increases natriuretic peptide expression and signaling. *J Am Coll Cardiol*. 2011;57:2273–2283.

32. Tsutsumi YM, Kawaraguchi Y, Horikawa YT, Niesman IR, Kidd MW, Chin-Lee B, Head BP, Patel PM, Roth DM, Patel HH. Role of Caveolin-3 and Glucose Transporter-4 in Isoflurane-induced Delayed Cardiac Protection. *Anesthesiology*. 2010;112:1136–1145.

33. Holland WL, Miller RA, Wang ZV, Sun K, Barth BM, Bui HH, Davis KE, Bikman BT, Halberg N, Rutkowski JM, Wade MR, Tenorio VM, Kuo MS, Brozinick JT, Zhang BB, Birnbaum MJ, Summers SA, Scherer PE. Receptor-mediated activation of ceramidase activity initiates the pleiotropic actions of adiponectin. *Nat Med*. 2011;17:55–63.

Supplement Materials

Materials and Methods:

All experiments were performed on adult male Cav-3 knockout mice (Cav-3KO) or male wild type littermate controls (WT). The experiments were performed in adherence with the National Institutes of Health Guidelines on the use of Laboratory Animals and were approved by the Thomas Jefferson University Committee on Animal Care. The authors had full access to and take full responsibility for the integrity of the data. All authors have read and agree to the manuscript as written.

Myocardial ischemia/reperfusion protocols: Mice were anesthetized with 2% isoflurane (total exposure time <5 minutes), and myocardial ischemia (MI) was produced by temporarily exteriorizing the heart (<1 minute) via a left thoracic incision and placing a 6-0 silk suture slipknot around the left anterior descending coronary artery[1]. Twenty minutes after MI, animals were randomized to receive either vehicle or globular domain of adiponectin (gAPN, 2 µg/g, ip)[1]. After 30 minutes of MI, the slipknot was released, and the myocardium was reperfused for 3 hours or 24 hours (cardiac function and infarct size only). All assays were performed using the tissue from ischemic/reperfused area or area-at-risk (AAR) identified with Evens blue negative staining as described below.

Determination of Cardiac Function: 24 hours after reperfusion, cardiac function was determined by echocardiography (VisualSonics VeVo 770 imaging system) as well as left ventricular (LV) catheterization methods before the chest was reopened [1, 2]. For echocardiography, mice were anesthetized with a 1.5% isoflurane and two-dimensional echocardiographic views of the mid-ventricular short axis were obtained at the level of the papillary muscle tips below the mitral valve (Vevo 770, VisualSonic, Toronto, Canada). LV fractional shortening (LVFS) and LV ejection fraction (LVEF) were calculated. For hemodynamic measurements, the right common

carotid artery of mice was cannulated with 1.2 French micro-manometer (Millar Instruments, Houston, TX). LV pressure, LV end-diastolic pressure (LVEDP), maximal and minimum values of the instantaneous first derivative of LV pressure (±dP/dtmax), and heart rate (HR) were measured by this catheter advanced into the LV cavity, and data was recorded and analyzed on a PowerLab System (AD Instruments Pty Ltd., Mountain View, CA).

Determination of Myocardial Infarct Size: At the end of the 24-hour reperfusion period, the ligature around the coronary artery was retied and 0.5 ml of 2% Evans blue dye was injected into the left ventricular cavity. The dye was circulated and uniformly distributed except in that portion of the heart previously perfused by the occluded coronary artery (area-at-risk, AAR). The heart was excised, frozen in -20° C, and sliced into 1 mm thick sections perpendicular to the long axis of the heart. Slices were incubated individually using a 24-well culture plate in 1% TTC in phosphate buffer at pH 7.4 at 37° C for 10 minutes, and photographed with a digital camera. The Evan's blue stained area (area-not-at-risk, ANAR), the TTC stained area (red staining, ischemic but viable tissue), and the TTC stained negative area (infarct myocardium) were digitally measured using an IP Lab Imagine Analysis Software (Version 3.6, Scanalytics, Fairfax, VA) with a custom-made script (Bio Vision Technologies, North Exton, PA). The myocardial infarct size was expressed as a percentage of infarct area over AAR.

Measurement of caspase-3 activity: Apoptotic cell death was determined by caspase-3 activation as described in our previous study[2]. Briefly, 3 hours after reperfusion, heart was removed and cardiac tissue from AAR was homogenized utilizing caspase lysis buffers (50mM HEPES PH 7.4, 0.1% Chaps, 5mM DTT, 0.1 mM EDTA, 0.1% Triton-X100). To each well of a 96-well plate, supernatant containing 200 µg of protein was loaded and incubated with 25 µg Ac-DEVD-_p_NA at

37° C for 1.5 hours. *p*NA was cleaved from DEVD by activated caspase-3, and the free pNA was quantified using a SpectraMax-Plus microplate spectrophotometer (Molecular Devices, Sunnyvale, CA) at 405 nm. Caspase-3 activity was expressed as nmol pNA/h/mg protein.

Determination of Total NOx Content in Cardiac Tissue: Cardiac tissue samples from AAR were rinsed, homogenized in deionized water (1:10, wt.vol^{-1}), and centrifuged at 14,000 x *g* for 10 minutes. The tissue NO and its *in vivo* metabolic products (NO_2 and NO_3) in the supernatant, collectively known as NOx, were determined using a chemiluminescence NO detector (SIEVER 280i NO Analyzer) as described in our previous study [3].

Quantification of Superoxide Production: Superoxide production in ischemic/reperfused heart tissue was measured by lucigenin-enhanced chemiluminescence as previously described [4]. Superoxide production was expressed as relative light units (RLU) per second per mg heart weight (RLU.mg^{-1}.s^{-1}).

Quantitation of Tissue Nitrotyrosine Content: Nitrotyrosine content in the ischemic/reperfused cardiac tissue, a footprint of *in vivo* peroxynitrite formation and a reliable index for nitrative stress [5,6], was determined using an ELISA method described in our previous publication [7]. The results were presented as pmol of nitrotyrosine/mg protein.

Immunoblotting: Protein from tissue homogenate was separated on SDS-PAGE gels, transferred to nitrocellulose membranes, and Western blotted with monoclonal antibody against iNOS, NOX-2, AMPK, pAMPK, ACC and pACC. Nitrocellulose membranes were then incubated with HRP-conjugated anti-mouse IgG antibody (1:2000, Cell Signaling) for 1 hour and the blot was developed with a Supersignal chemiluminescence detection kit (Pierce). The immunoblotting was visualized with a Kodak Image Station 400 and the blot densities were analyzed with Kodak 1D software.

<u>Sucrose density membrane fractionation</u>: Whole hearts were homogenized in Triton X-100 with a tissue grinder followed by sonication. The resulting cell lysates were mixed with equal amounts of 80% sucrose in MBS, yielding a 40% sucrose concentration. Lysates containing the 40% sucrose were loaded at the bottom of an ultracentrifuge tube, and overlaid with 4 ml each of 35% and 5% sucrose in MBS. The gradient was centrifuged at 175,000 g with a Beckman SW41Ti rotor (Beckman Instruments, Fullerton, CA, USA) for 24 hours at 4°C. The resulting gradient fractions were analyzed by collecting twelve 1-ml fractions from the bottom of the gradient. Fractions 4-6 were buoyant membrane fractions (BFs) enriched in caveolae. Fractions 9-12 were defined as non-buoyant fractions (non-BFs). The fractions were subjected to co-immunoprecipitation or Western blot analysis as described in detail below.

Adult mouse cardiomyocyte culture and confocal microscopic analysis: Adult mouse cardiomyocytes were isolated as previously described[1]. Cells were washed and fixed with 4% paraformaldehyde/PBS. The samples were pretreated with 10% fetal bovine serum in phosphate buffered saline for 30 minutes. After PBS rinsing, rabbit anti-mouse Cav-3 or goat anti-mouse APN receptor 1 (AdipoR1) antibody (1:200) in the same blocking solution were added to the sample and incubated for 1 hour. Nonimmune rabbit IgG and goat IgG were included as controls. Following five 5-minute washes with blocking solutions, tetramethyl rhodamine (TRITC)-conjugated chicken anti-rabbit IgG and Cy5-conjugated donkey anti-goat IgG (Abcam, Cambridge, MA.1:200) were added, and incubated for 30 minutes. After washing with phosphate-buffered saline, coverslips were mounted using an anti-fade solution (KPL, Gaithersburg, MD). Samples were examined with a FV1000 confocal microscope (Olympus, Tokyo, Japan), and images were processed with the Fluoview software (Olympus). More than 100 cells were inspected per experiment, and cells with typical morphology are presented.

Plasmid production, cell transfection and co-immunoprecipitation: Full-length AdipoR1 (residues 1–375, AdipoR1-F) and truncated AdipoR1 (AdipoR1-T), including AdipoR1-T$^{1-230}$, AdipoR1-T$^{1-215}$, AdipoR1-T$^{316-375}$, AdipoR1-T$^{336-375}$ were generated by PCR using the wild type mouse AdipoR1 cDNA (gift from Dr. Lily Dong, Department of Pharmacology, University of Texas Health Science Center, San Antonio, TX) as a template, and cloned into pcDNA3.1 with myc-tag. Full length Cav-3 (residue 1-151, Cav-3F) and truncated Cav-3 (Cav-3T), including Cav-3T$^{1-74}$, Cav-3T$^{1-54}$, Cav-3T$^{54-74}$, and Cav-3T$^{74-151}$ were generated by PCR using the wild-type mouse Cav-3 cDNA as a template, and cloned into the p3XFLAG. Human embryonic kidney 293T cells were grown to 90% confluence in 6-well dishes, and transfected with plasmids encoding AdiopR1-F, AdipoR1-T, Cav-3F, Cav-3T (2 μg DNA), or empty vectors (p3XFLAG or pcDNA3.1) by Lipofectamine 2000 Reagent per manufacturer's instructions (Invitrogen, Carlsbad, CA). Cells were incubated with lipid–DNA complexes in serum-free DMEM for 8 hours. Following transfection, cells were washed twice with PBS, and cultured in medium containing 10% serum till confluence. Cells were scraped into 1 ml of ice cold RIPA lysis buffer (1XTBS, 1% Nonidet p-40, 0.5% sodium deoxycholate, 0.1% SDS, 0.004% sodium azide, 1mM Na$_3$VO$_4$, 0.5mM EDTA, supplemented with protease inhibitor cocktail). After sonication on ice, debris was removed by centrifugation at 12,000 g for 10 minutes. Lysates were pre-cleared by incubation with 30μl of a 1:1 slurry of Protein G-Sepharose for 30 minutes at 4°C on a rotating wheel. The bead pellet was discarded, and the supernatant was used for immunoprecipitation. 4μg of anti-flag IgG or Anti-myc IgG (Sigma) was added to the lysates and incubated overnight at 4°C on a rotating wheel. Irrelative anti-mouse IgG served as negative control. Fresh Protein G-Sepharose (30μl) was then added, and samples were incubated for 4 hours at 4°C. Immune complexes were collected by centrifugation, washed three times sequentially with each of the

following solutions: RIPA buffer, buffer A (50mM pH7.5 Tris, 500mM NaCl, 1mM EDTA and 0.2% Triton X-100) and buffer B (10mM pH7.5 Tris and 0.2% Triton X-100). Complexes were then disrupted by boiling in elusion buffer (Pierce).

Statistical analysis: All values in the text and figures are presented as means±SEM of *n* independent experiments. All data (except Western blot density) were subjected to two-way ANOVA followed by Bonferoni correction for *post-hoc* test. Western blot densities were analyzed with the Kruskal-Wallis test followed by Dunn's post-hoc test. Probabilities of 0.05 or less were considered to be statistically significant.

Reference List

(1) Tao L, Gao E, Jiao X, Yuan Y, Li S, Christopher TA, Lopez BL, Koch W, Chan L, Goldstein BJ, Ma XL. Adiponectin cardioprotection after myocardial ischemia/reperfusion involves the reduction of oxidative/nitrative stress. *Circulation* 2007 March 20;115(11):1408-16.

(2) Tao L, Gao E, Bryan NS, Qu Y, Liu HR, Hu A, Christopher TA, Lopez BL, Yodoi J, Koch WJ, Feelisch M, Ma XL. Cardioprotective effects of thioredoxin in myocardial ischemia and reperfusion: Role of S-nitrosation. *PNAS* 2004 July 26;101:11471-6.

(3) Gao F, Gao E, Yue TL, Ohlstein EH, Lopez BL, Christopher TA, Ma XL. Nitric oxide mediates the antiapoptotic effect of insulin in myocardial ischemia-reperfusion: the roles of PI3-kinase, Akt, and endothelial nitric oxide synthase phosphorylation. *Circulation* 2002 March 26;105(12):1497-502.

(4) Lund DD, Faraci FM, Miller FJ, Jr., Heistad DD. Gene transfer of endothelial nitric oxide synthase improves relaxation of carotid arteries from diabetic rabbits. *Circulation* 2000 March 7;101(9):1027-33.

(5) Aulak KS, Koeck T, Crabb JW, Stuehr DJ. Dynamics of protein nitration in cells and mitochondria. *Am J Physiol Heart Circ Physiol* 2004 January 1;286(1):H30-H38.

(6) Kuhn DM, Sakowski SA, Sadidi M, Geddes TJ. Nitrotyrosine as a marker for peroxynitrite-induced neurotoxicity: the beginning or the end of the end of dopamine neurons? *J Neurochem* 2004 May;89(3):529-36.

(7) Ma XL, Gao F, Nelson AH, Lopez BL, Christopher TA, Yue TL, Barone FC. Oxidative inactivation of nitric oxide and endothelial dysfunction in stroke-prone spontaneous hypertensive rats. *J Pharmacol Exp Ther* 2001 September;298(3):879-85.
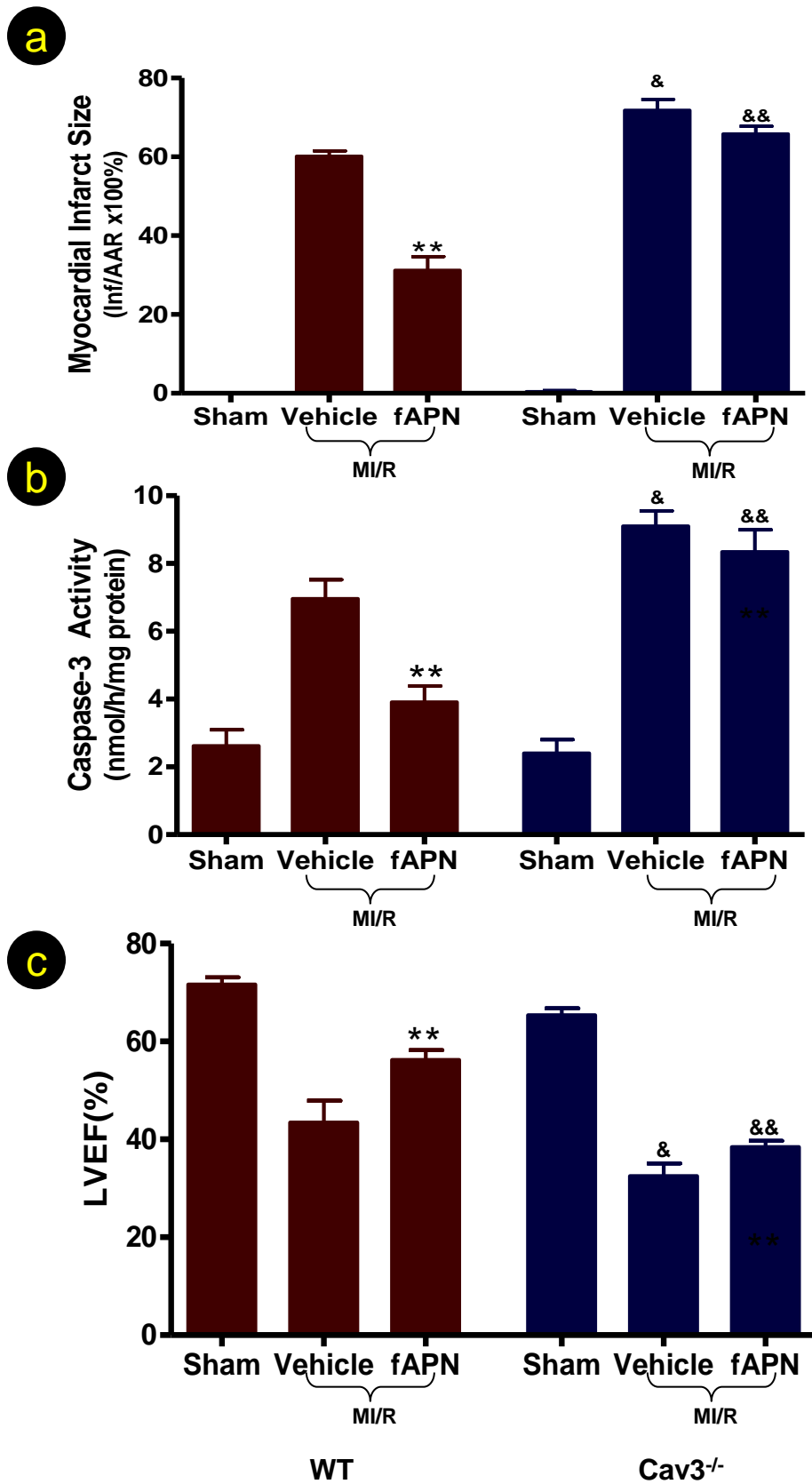
Figure I. Knockout of Cav-3 blocked cardioprotective effects of full length APN (10 μg/g).
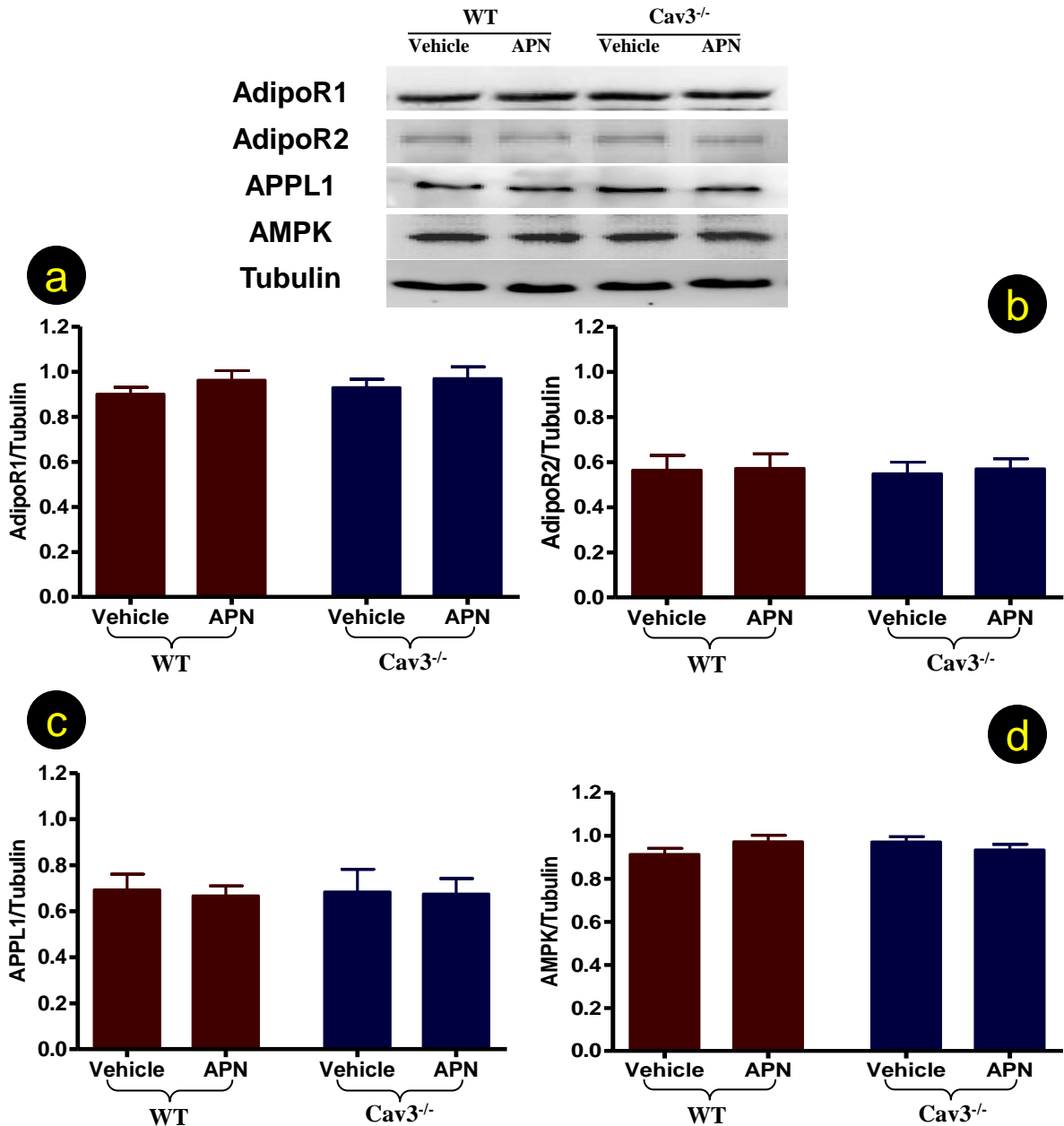
Figure II. Knockout of Cav-3 had no significant effect on key APN signaling molecules including AdipoR1 (A), AdipoR2 (B), APPL1 (C) and AMPK (D). Top insert: typical Western blots; Bar graphs: summary data from at least 6 heart/group.
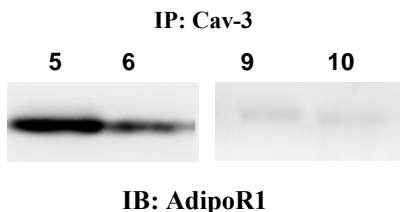

Figure III. AdipoR1/Cav-3 complex was detected in fractions 5 and 6, but no in fractions 9 and 10.

a

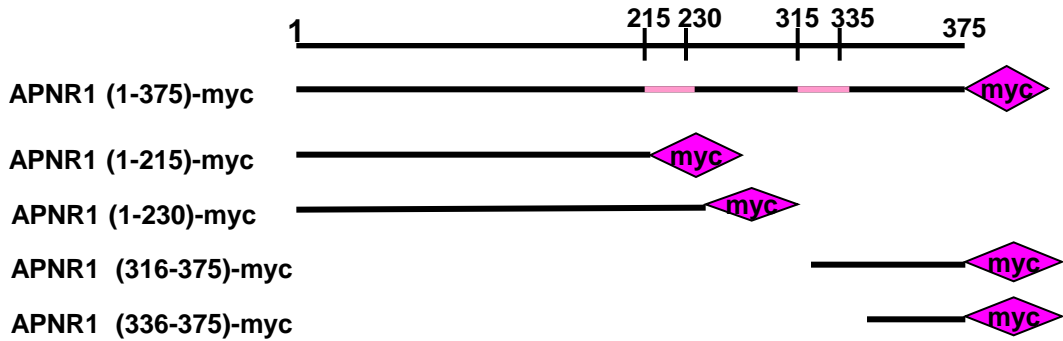AdipoR1 220-228 FVPWLYYSF
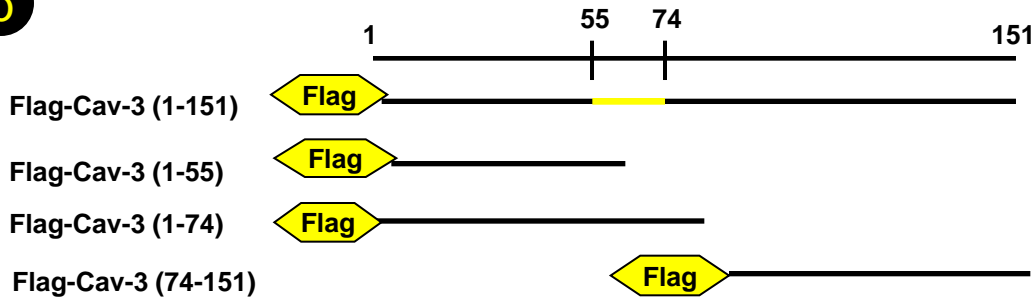AdipoR1 325-333 FFPGKFDIW

1   215 230   315 335   375

APNR1 (1-375)-myc

APNR1 (1-215)-myc

APNR1 (1-230)-myc

APNR1 (316-375)-myc

APNR1 (336-375)-myc

b

1   55   74   151

Flag-Cav-3 (1-151)

Flag-Cav-3 (1-55)

Flag-Cav-3 (1-74)

Flag-Cav-3 (74-151)

Figure IV. A diagram depicts the truncation mutations of AdipoR1 (a) and Cav-3 (b).

WT   Cav-3KO

peNOS

eNOS

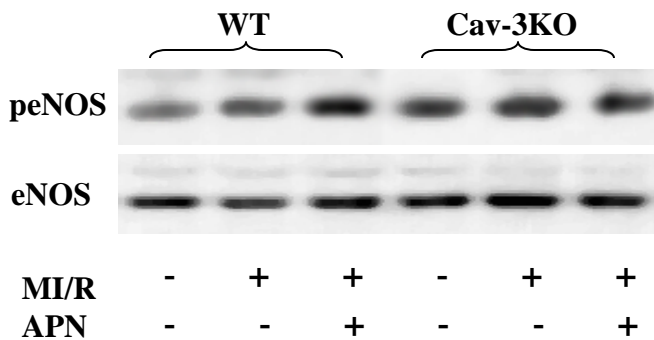| MI/R | - | + | + | - | + | + |
| APN | - | - | + | - | - | + |

Figure V. Treatment with APN significantly increased eNOS phosphorylation in WT mice (lane 3 vs. lane 1). Basal level of eNOS phosphorylation was increased in Cav-3KO mice (lane 4 vs. lane 1). However, treatment with APN failed to increase eNOS phosphorylation in Cav-3KO mice (lane 6 vs. lane 4).